

Recent Developments in the Thermally Activated Delayed Fluorescence of Fullerenes

Carlos Baleizão and Mário N. Berberan-Santos

Centro de Química-Física Molecular and IN, IST-UTL, 1049-001 Lisboa, Portugal

Recent developments in fundamental aspects and applications of the thermally activated delayed fluorescence (TADF) displayed by fullerenes are presented. It is shown that from the analysis of steady-state data, time-resolved data, or a combination of both, it is possible to determine several important photophysical parameters. Outstanding temperature and oxygen sensors based on the TADF effect exhibited by fullerene C₇₀ are also briefly discussed.

Introduction

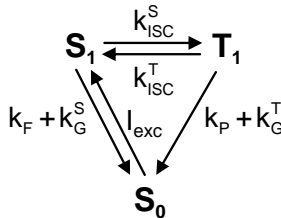
The discovery of fullerenes in 1985 (1) and their production in macroscopic amounts after 1990 (2) opened a new field of research. Applications of fullerenes in areas like energy, materials, biopharmaceuticals, optics, and electronics, started to appear in the last years. The most common fullerenes are C₆₀ and C₇₀, three-dimensional carbon structures that can be viewed either as large carbon molecules or as tiny nanoparticles with well defined composition and shape. Their photophysical and photochemical properties result from the large number of delocalized pi electrons and also from the high symmetry and curvature of the structures. The photophysics of fullerenes has been the subject of considerable investigation (3–5). One of the most characteristic and (to us) interesting photophysical properties of C₆₀, C₇₀, and derivatives, first observed in our group, is a second mechanism for fluorescence, which is called thermally activated delayed fluorescence (TADF). This phenomenon that occurs in a few fluorescent molecules is usually quite weak, however in the case of fullerenes it is very strong, especially for C₇₀. Herein, we briefly review recent developments in fundamental aspects and applications of the TADF of fullerenes.

Thermally Activated Delayed Fluorescence: Basic Aspects

Molecular fluorescence can take place by two different unimolecular mechanisms: Prompt fluorescence (PF) and thermally activated delayed fluorescence (TADF) (6,7). In the PF mechanism, emission occurs after S_n←S₀ absorption and excited state relaxation to S₁. The TADF mechanism takes place via the triplet manifold: After excitation and once attained S₁, intersystem crossing (ISC) to the triplet manifold (T₁ or a higher triplet) occurs, followed by a second ISC from T₁ back to S₁, and by fluorescence emission proper. The cycle S₁→T₁→S₁ may repeat itself a number of times before fluorescence finally takes place. TADF is significant only when the quantum yield of triplet formation (Φ_T) and the quantum yield of singlet formation (Φ_S) are both high (8). This in turn implies a small energy gap between S₁ and T₁ (ΔE_{ST}), a long T₁ lifetime, and not too low

a temperature (8). For a given fluorophore, TADF is usually much weaker than its PF. Although known for many years, TADF continues to be a relatively rare phenomenon (9). The remarkable photophysical properties of fullerene C₇₀, specifically the Φ_T very close to one (10), the small ΔE_{ST} gap (11) and the long intrinsic phosphorescence lifetime (12), led to the discovery of an exceptionally strong TADF in this molecule (8). C₆₀ (13) and some C₆₀ derivatives (14,15), as well as one C₇₀ derivative (16), also exhibit TADF, but weaker than that of C₇₀.

The simplest model for thermally activated delayed fluorescence in the condensed phases is a three-state system that can be represented by the following kinetic scheme,



Scheme 1. Kinetic scheme for TADF

where I_{exc} is the excitation intensity, k_F and k_P are the radiative rate constants for fluorescence and phosphorescence, respectively, k_G^S and k_G^T are the nonradiative rate constants for deactivation to the ground state (internal conversion from S₁ and intersystem crossing from T₁, respectively), and k_{ISC}^S and k_{ISC}^T are the intersystem crossing rate constants for singlet-to-triplet and triplet-to-singlet conversion, respectively. Owing to the relative energies of S₁ and T₁, the triplet-to-singlet ISC rate constant always corresponds to an activated process that is strongly temperature dependent (6,8,17):

$$k_{ISC}^T = A \exp\left(-\frac{\Delta E_{ST}}{RT}\right) \quad [1]$$

For strong TADF to occur, the following inequalities need to be met: $k_{ISC}^S \gg k_F + k_G^S$ and $k_{ISC}^T \gg k_P + k_G^T$. In most cases it is also observed that $k_{ISC}^S \gg k_{ISC}^T$ and $k_G^T \gg k_P$.

The time-evolution of the S₁ and T₁ populations is given by the following coupled equations (18), where for simplicity the square brackets representing the concentrations are omitted:

$$S_1(t) = I_{exc}(t) \otimes \exp(-t/\tau_F) + k_{ISC}^T T_1(t) \otimes \exp(-t/\tau_F) \quad [2]$$

$$T_1(t) = k_{ISC}^S S_1(t) \otimes \exp(-t/\tau_P) \quad [3]$$

where \otimes stands for the convolution between two functions, $f \otimes g = \int_0^t f(u) g(t-u) du$, $\tau_F = 1/(k_F + k_G^S + k_{ISC}^S)$ is the (prompt) fluorescence lifetime, and $\tau_P = 1/(k_P + k_G^T + k_{ISC}^T)$ is called here the phosphorescence lifetime. These two lifetimes only have direct experimental meaning in the absence of reversibility, otherwise fluorescence and

phosphorescence no longer have single exponential decays, as will be discussed below. The low temperature phosphorescence lifetime is $\tau_p^0 = 1/(k_p + k_G^T)$. For rigid molecules, the temperature dependence of k_G^T is mainly dictated by external effects, i.e., interactions with the solvent and other solutes present, e.g. oxygen and impurities, and therefore k_G^T is expected to change moderately with temperature in a deoxygenated and photochemically inert solid medium (19).

Scheme 1 is isomorphous to the monomer-excimer scheme, and has therefore the same general solution. This solution can be obtained by insertion of Eq. (3) into Eq. (2),

$$S_1(t) = I_{exc}(t) \otimes \exp(-t/\tau_F) + k_{ISC}^S k_{ISC}^T S_1(t) \otimes \exp(-t/\tau_P) \otimes \exp(-t/\tau_F) \quad [4]$$

and then by repeated substitution of the left hand side on the right hand side (17),

$$\begin{aligned} S_1(t) = & I_{exc}(t) \otimes \exp(-t/\tau_F) + k_{ISC}^S k_{ISC}^T I_{exc}(t) \otimes \exp(-t/\tau_F) \otimes \exp(-t/\tau_P) \otimes \exp(-t/\tau_F) + \\ & + (k_{ISC}^S k_{ISC}^T)^2 I_{exc}(t) \otimes \exp(-t/\tau_F) \otimes \exp(-t/\tau_P) \otimes \exp(-t/\tau_F) \otimes \exp(-t/\tau_P) \otimes \exp(-t/\tau_F) + \dots \end{aligned} \quad [5]$$

hence the first term for the singlet decay can be associated with prompt fluorescence (zero $S_1 \rightarrow T_1 \rightarrow S_1$ cycles), and the remaining terms with delayed fluorescence, the n th term resulting from $n-1$ $S_1 \rightarrow T_1 \rightarrow S_1$ cycles. Analogous results can be obtained for the triplet decay. The singlet decay, Eq. (5), simplifies into a sum of two exponentials of time, and the triplet decay into a difference of the same two exponentials (20):

$$S_1(t) = \frac{S_1(0)}{\lambda_2 - \lambda_1} [(\lambda_2 - X) \exp(-\lambda_1 t) + (X - \lambda_1) \exp(-\lambda_2 t)] \quad [6]$$

$$T_1(t) = \frac{k_{ISC}^S S_1(0)}{\lambda_2 - \lambda_1} [\exp(-\lambda_1 t) - \exp(-\lambda_2 t)] \quad [7]$$

where

$$\lambda_{1,2} = \frac{1}{2} \left\{ X + Y \mp \sqrt{(Y - X)^2 + 4k_{ISC}^S k_{ISC}^T} \right\} \quad [8]$$

with

$$X = \frac{1}{\tau_F} \quad [9]$$

$$Y = \frac{1}{\tau_P^0} + k_{ISC}^T \quad [10]$$

When inter-conversion between the singlet and triplet emissive states occurs many times before photon emission or nonradiative decay can take place, a fast pre-equilibrium

between S_1 and T_1 is established, and for sufficiently long times both S_1 and T_1 decay with a common rate constant given by (21)

$$k = \frac{1}{\tau_{DF}} = k_G^T + (1 - \Phi_T) k_{ISC}^T \quad [11]$$

where Φ_T is the quantum yield of triplet formation, $\Phi_T = k_{ISC}^S / (k_F + k_G^S + k_{ISC}^S)$, and τ_{DF} is the delayed fluorescence (and phosphorescence) lifetime.

The fluorescence quantum yield is given by

$$\Phi_F = \Phi_{PF} + \Phi_{DF} \quad [12]$$

where the quantum yields for prompt Φ_{PF} and delayed Φ_{DF} fluorescence obey the following relation (8)

$$\frac{\Phi_{DF}}{\Phi_{PF}} = \frac{I_{DF}}{I_{PF}} = \frac{1}{\frac{1}{\Phi_S \Phi_T} - 1} \quad [13]$$

and the quantum yield of singlet formation is defined by

$$\Phi_S = \frac{k_{ISC}^T}{k_P + k_G^T + k_{ISC}^T} \quad [14]$$

For strong TADF to occur the cycle $S_1 \rightarrow T_1 \rightarrow S_1$ must repeat a number of times before photon emission or nonradiative decay can take place.

The average number of cycles \bar{n} is given by

$$\bar{n} = \sum_{n=0}^{\infty} n p_n = \frac{\Phi_T \Phi_S}{1 - \Phi_T \Phi_S} = \frac{1}{\frac{1}{\Phi_T \Phi_S} - 1} = \frac{1}{\frac{1}{\Phi_T} \left(1 + \frac{1}{k_{ISC}^T \tau_P^0} \right) - 1} \quad [15]$$

Comparison of Eqs. (15) and (13) gives immediately

$$\frac{\Phi_{DF}}{\Phi_{PF}} = \frac{I_{DF}}{I_{PF}} = \bar{n} \quad [16]$$

and, using Eq. (12),

$$\frac{\Phi_F}{\Phi_{PF}} = \frac{I_F}{I_{PF}} = 1 + \bar{n} \quad [17]$$

hence the increase in fluorescence intensity owing to TADF is a direct measure of the average number of $S_1 \rightarrow T_1 \rightarrow S_1$ cycles performed. This result is easy to understand, as each return from T_1 to S_1 brings a new opportunity for fluorescence emission.

In the absence of reversibility, $\bar{n} = 0$. On the other hand, for the fastest possible excited state equilibration ($k_{\text{ISC}}^{\text{T}} \rightarrow A$, $\Phi_{\text{S}} \cong 1$) one has

$$\bar{n} \cong \frac{1}{\frac{1}{\Phi_{\text{T}}} - 1} \quad [18]$$

Therefore, the maximum possible fluorescence intensification factor, Eq. (17), is $I/(I - \Phi_{\text{T}})$. Using the following set of data, obtained for fullerene C_{70} dispersed in polystyrene (17,22,23): $\Phi_{\text{T}} = 0.99$, $\tau_{\text{F}} = 630$ ps, $\tau_{\text{P}}^0 = 28$ ms, $A = 8 \times 10^7 \text{ s}^{-1}$, $\Delta E_{\text{ST}} = 29 \text{ kJ mol}^{-1}$, the maximum average number of cycles is estimated to be 99, and the maximum fluorescence intensification factor to be 100.

Several methods of TADF data analysis exist. The classical one, due to Parker (6), combines steady-state delayed fluorescence and phosphorescence intensities for the determination of ΔE_{ST} . This method was successfully applied to C_{70} (8). Nevertheless, in many cases it is not possible or convenient to measure the phosphorescence, and it is precisely in these cases that a non-spectroscopic method for the estimation of ΔE_{ST} becomes valuable. Furthermore, photophysical parameters other than ΔE_{ST} are of interest and can be extracted from experimental TADF data by other methods.

From the steady-state data, and for the purpose of curve fitting, Eq. (14) can be conveniently rewritten as (8)

$$\ln \left[\frac{I_{\text{PF}}}{I_{\text{DF}}} - \left(\frac{1}{\Phi_{\text{T}}} - 1 \right) \right] = \ln \left[\frac{1}{\Phi_{\text{T}}} \left(\frac{1}{\Phi_{\text{S}}^{\infty}} - 1 \right) \right] + \frac{\Delta E_{\text{ST}}}{RT} \quad [19]$$

where

$$\Phi_{\text{S}}^{\infty} = \frac{1}{\frac{1}{A\tau_{\text{P}}^0} + 1} \quad [20]$$

and from a fit to steady-state data arranged in the above form (8) it is possible to recover ΔE_{ST} , Φ_{T} , and Φ_{S}^{∞} , assuming that Φ_{S}^{∞} is temperature independent. Alternatively, a non-linear curve fitting can also be carried out.

Concerning the time-resolved data, the time constant for the TADF lifetime is given by (17)

$$\lambda_1 = \frac{1}{\tau_{\text{P}}^0} + k_{\text{ISC}}^{\text{T}} (1 - \Phi_{\text{T}}) \quad [21]$$

Using Eq. (1), Eq. (21) becomes

$$\lambda_1 = \frac{1}{\tau_{\text{P}}^0} + B \exp \left(-\frac{\Delta E_{\text{ST}}}{RT} \right) \quad [22]$$

where $B = (1 - \Phi_T)A$. From a nonlinear fit to the temperature dependence of the fluorescence long component (delayed fluorescence lifetime) using Eq. (22), and assuming that τ_p^0 is temperature independent, it is possible to recover ΔE_{ST} , B and τ_p^0 from time-resolved measurements. Nevertheless, and owing to parameter correlation, it is preferable to fix ΔE_{ST} at the steady-state value (obtained with Eq. (19)). In this way, A and τ_p^0 can be extracted from the temperature dependence of the delayed fluorescence lifetime (17). An alternative procedure is to rewrite Eq. (22) as

$$\ln\left(\lambda_1 - \frac{1}{\tau_p^0}\right) = \ln B - \frac{\Delta E_{ST}}{RT} \quad [23]$$

and to search for the value of τ_p^0 that gives the best straight line.

A new method of analysis combines steady-state and time-resolved (delayed fluorescence) data in the same plot (17)

$$\tau_{DF} = \tau_p^0 - \left(\frac{1}{\Phi_T} - 1\right) \tau_p^0 \frac{I_{DF}}{I_{PF}} \quad [24]$$

This linear plot yields Φ_T and τ_p^0 , assuming τ_p^0 to be temperature independent. If τ_p^0 is already known, Φ_T can be directly obtained from Eq. (24).

In conclusion, from steady-state and time-resolved data, it is in principle possible to obtain Φ_T , A , ΔE_{ST} , and τ_p^0 using several methods.

Sensing Applications

Optical chemical sensors allow the continuous recording of the concentration of chemical species (like O_2 , CO_2 , or several ions) and physical parameters (pressure, temperature, etc.) and therefore have a wide range of applications. Among the many optical methods which are employed for sensing, fluorescence has attracted special attention because it is highly sensitive and versatile.

In fluorescence, the sample can be both excited and measured optically. Therefore, fluorescence-based sensors, not requiring contact with the medium during measurement, are advantageous compared to contact sensors in applications where electromagnetic noise is strong or it is physically difficult to connect a wire. Further advantages of the molecular fluorescence sensors are the very fast response, the reversibility and the space resolution that can go from the macroscale (fluorescent paints) down to the nanoscale (fluorescence microscopy). These properties also overcome the limitations of the electrochemical sensors (difficult to miniaturize, invasive technique and limited to discrete points).

Temperature Measurement

There are several temperature sensors based on molecular optical properties, namely luminescence. The use of fiber optics in conjugation with phosphors, whose

luminescence lifetime changes with temperature, is a well established method (24). More recently, several studies have been devoted to fluorescence molecular thermometry.

There is presently a need for optical sensors covering a wide temperature range, say from 100 °C to 250 °C. The common luminescence temperature sensors used currently are based on metallic complexes (Ru, Pt, Pd, etc.) whose intensity almost invariably decreases with a temperature increase owing to thermally-activated quenching processes, with working range temperatures below 100 °C. The high thermal stability and the unique photophysical properties of fullerenes make these molecules well placed to fulfil this need.

The discovery (8) of TADF in fullerene C₇₀ was the first step for the development of temperature sensors based on the delayed fluorescence of fullerenes. The study was carried out in a degassed solution of liquid paraffin. The intensity of the non degassed solution is independent of temperature, and is entirely due to prompt fluorescence. The rise with temperature observed in the degassed solutions results from the increasing contribution of delayed fluorescence to the total intensity. The delayed fluorescence obtained at 70 °C in degassed medium is 50 times stronger than the PF.

The reversibility of the C₇₀/paraffin system was also evaluated. Up to 70 °C, the system shows total reversibility; however for higher temperatures the reversibility is lost. Another drawback is the liquid nature of the system. For these reasons, we developed a series of polymer films with C₇₀ molecularly dispersed in them (22,23).

To study the influence of the polymer matrix structure on the photophysics and TADF of C₇₀, three polymers were selected: Polystyrene (PS), poly(tert-butyl methacrylate) (PtBMA), and poly(1-vinylnaphthalene) (P1VN). The films were prepared by evaporating a toluene solution of C₇₀ and polymer on a quartz plate. After film formation and drying, the plates were placed in a quartz cell that was degassed at room temperature and afterwards sealed. All the films exhibited absorption spectra similar to that of C₇₀ in toluene (for PS and P1VN) or methylcyclohexane (for PtBMA). These results are in agreement with a molecular dispersion of C₇₀ in the polymeric films.

Without degassing, the fluorescence intensity of C₇₀/PS films is temperature-independent. After degassing, a 22-fold enhancement of the room-temperature fluorescence was observed. This enhancement is a consequence of the additional contribution of delayed fluorescence (DF) to the overall emission. Heating of the sample to 100 °C (a temperature at which the DF is 70 times higher than the PF) shows that the fluorescence of C₇₀ has a strong temperature dependence. The C₇₀/PS film exhibits full reversibility and fluorescence intensity cycles without hysteresis. The results exhibited a high degree of reproducibility.

Identical temperature cycles were carried out for the C₇₀/P1VN and C₇₀/PtBMA films. Responses similar to that of the C₇₀/PS film were observed. The films exhibit very good reversibility in the thermal cycles and high reproducibility. The maximum I_{DF}/I_{PF} value was obtained at 100 °C with the C₇₀/PtBMA system.

The temperature sensitivity of fluorescence intensity was also calculated, and can be defined either as the variation of the fluorescence quantum yield with temperature, which is the absolute sensitivity S_A (Eq. (25)), or as the relative variation of the fluorescence quantum yield with temperature, which is the relative sensitivity S_R (Eq. (26)).

$$S_A = \frac{d\Phi_F}{dT} \quad [25]$$

$$S_R = \frac{1}{\Phi_F} \frac{d\Phi_F}{dT} = \frac{d \ln \Phi_F}{dT} \quad [26]$$

We will use the relative sensitivity as it directly reflects the relative variation of the fluorescence intensity. The C₇₀/polymer systems have some of the highest temperature sensitivities known over a broad temperature range (25). In order to define a useful working range, a minimum value of 0.5 % K⁻¹ for S_R is assumed. With this value, the lower temperature limit is -80 °C for all polymers. At the other end of the scale, the C₇₀/PtBMA system displays the highest high-temperature limit (140 °C), whereas for the other two polymers the upper limit is 110 °C.

The C₇₀-based luminescence thermometer is a new development in the molecular thermometry field owing to the possibility of using a highly sensitive probe that covers not only both the low temperature and the physiological temperature ranges, but that can also be used for temperatures well above 100 °C.

Oxygen Sensing

A variety of devices and sensors based on molecular optical properties has been developed for the measurement of molecular oxygen. Many optical oxygen sensors are composed of organic dyes, transition metal complexes and metalloporphyrins immobilized in oxygen permeable materials (26). There is still a need for optical sensors that can respond to very low levels of oxygen. The TADF effect in the fullerenes is very sensitive to the presence of oxygen (8), leading to a very efficient quenching of the intensity and lifetime of TADF. Due to this ultra sensitivity to oxygen, fullerenes are useful for sensing oxygen in low concentrations.

In a recent paper, fullerene C₇₀ was embedded in two highly permeable polymer membranes, an organosilica, and an ethyl cellulose and used as optical sensor for trace amounts of oxygen with detection limits in the ppb range (27).

The highest O₂ permeabilities are displayed by silica-based polymers. But in all reports of sol-gels doped with unfunctionalized fullerenes, the fullerene was partially aggregated owing to formation of small clusters (28). These aggregates show largely reduced fluorescence intensities and lifetimes as a result of self-quenching. We have been able to incorporate C₇₀ into an organically modified silica without significant aggregation by using a monomer where one alkoxy group is replaced by a phenyl ring (28). Organosilicas (OS) are less polar and thus more compatible with fullerenes. Ethyl cellulose 49% (EC) also is a highly permeable matrix for oxygen sensing. C₇₀ is compatible with this matrix.

The sensitivity to oxygen was investigated by time-domain fluorescence lifetime imaging. The DF lifetimes exceed 20 ms in the absence of oxygen at room temperature and below, and result in an extreme sensitivity to oxygen. The response is instantaneous (<0.1 s). The fluorescence is most pronounced at 120 °C, and C₇₀ still shows DF lifetimes greater than 5 ms. The temperature dependence of the sensitivity is therefore the result of three effects: 1) an increase of Φ_{DF}, 2) a decrease of the DF lifetime, and 3) a higher collision rate of O₂. The Stern-Volmer constants depend on temperature in a nonlinear way and both systems display detection limits (defined at 1% quenching) more than one order of magnitude better than state-of-the-art probes.

The response of the matrices is fully reversible over many hundreds of times and showed no detectable degradation after three months of storage at room temperature in the dark on air. In conclusion, we developed an optical oxygen sensor that is especially

suiting for sensing oxygen down to the ppb range and also at high temperatures. The method makes use of the TADF of fullerene C₇₀ dissolved in appropriate polymers. It enables, for the first time, the optical sensing and imaging of oxygen at the ppbv level, and thus has a large potential (29).

Concluding Remarks

In this paper, recent results obtained by the authors in the field of fullerene photophysics were reviewed with an emphasis on thermally activated delayed fluorescence. It was shown that fullerenes display a strong TADF effect, which can be used to determine several photophysical parameters. This effect also allows the use of fullerenes as temperature and oxygen optical sensors under extreme conditions [high temperatures (> 100 °C) or low oxygen concentration (< 1 ppmv)].

In spite of the work already carried out, knowledge of the photophysics of fullerenes and derivatives is still incomplete, and much remains to be done in this area and in the field of optical sensor systems incorporating fullerenes.

Acknowledgments

This work was supported by Fundação para a Ciência e a Tecnologia (FCT, Portugal) and POCI 2010 (FEDER) within project PTDC/ENR/64909/2006.

References

1. H. W. Kroto, J. R. Heath, S. C. O'Brien, R. F. Curl, and R. E. Smalley, *Nature* **318**, 162 (1985).
2. W. Krätschmer, K. Fostiropoulos, and D. R. Huffman, *Nature* **347**, 354 (1990).
3. C. S. Foote, *Top. Curr. Chem.* **169**, 347 (1994).
4. Y. P. Sun, in *Molecular and Supramolecular Photochemistry*, vol. 1, *Organic Photochemistry*. V. Ramamurthy and K. S. Shanze, Editors, p. 325, Marcel Dekker, NY (1997).
5. Y. P. Sun, J. E. Riggs, Z. Guo, and H. W. Rollins, in *Optical and Electronic Properties of Fullerenes and Fullerene-Based Materials*, J. Shinar, Z. V. Vardeny, and Z. H. Kafafi, Editors, p. 43, Marcel Dekker, NY (2000).
6. C. A. Parker, *Photoluminescence of Solutions*, Elsevier, Amsterdam (1968).
7. B. Valeur, *Molecular Fluorescence: Principles and Applications*, Wiley-VCH, Weinheim (2002).
8. M. N. Berberan-Santos and J. M. M. Garcia, *J. Am. Chem. Soc.* **118**, 9391 (1996).
9. C. Baleizão and M. N. Berberan-Santos, *Ann. N. Y. Acad. Sci.* **1130**, 224 (2008).
10. J. W. Arbogast and C. S. Foote, *J. Am. Chem. Soc.* **113**, 8886 (1991).
11. S. M. Argentine, K. T. Kotz, and A. H. Francis, *J. Am. Chem. Soc.* **117**, 11762 (1995).
12. M. R. Wasielewski, M. P. O'Neil, K. R. Lykke, M. J. Pellin, and D.M. Gruen, *J. Am. Chem. Soc.* **113**, 2774 (1991).
13. F. A. Salazar, A. Fedorov, and M. N. Berberan-Santos, *Chem. Phys. Lett.* **271**, 361 (1997).
14. B. Gigante, C. Santos, T. Fonseca, M. J. M. Curto, H. Luftmann, K. Bergander, and M. N. Berberan-Santos *Tetrahedron* **55**, 6175 (1999).

15. S. M. Anthony, S. M. Bachilo, and R. B. Weisman, *J. Phys. Chem. A* **104**, 10674 (2003).
16. S. M. Bachilo, A. F. Benedetto, R. B. Weisman, J. R. Nossal, and W. E. Billups, *J. Phys. Chem. A* **104**, 11265 (2000).
17. C. Baleizão and M. N. Berberan-Santos, *J. Chem. Phys.* **126**, 204510 (2007).
18. M. N. Berberan-Santos and J. M. G. Martinho, *Chem. Phys.* **164**, 259 (1992).
19. W. E. Graves, R. H. Hofeldt, and S. P. McGlynn, *J. Chem. Phys.* **56**, 1309 (1972).
20. J. B. Birks, *Photophysics of Aromatic Molecules*, Wiley, London (1970).
21. M. Rae and M. N. Berberan-Santos, *Chem. Phys.* **280**, 283 (2002).
22. C. Baleizão and M. N. Berberan-Santos, *J. Fluoresc.* **16**, 215 (2006).
23. C. Baleizão, S. Nagl, S. M. Borisov, M. Schäferling, O. S. Wolfbeis, and M. N. Berberan-Santos, *Chem. Eur. J.* **13**, 3643 (2007).
24. K. T. Grattan and Z. Y. Zhang, *Fiber Optic Fluorescence Thermometry*, Chapman and Hall, London (1995).
25. O. S. Wolfbeis, *Anal. Chem.* **76**, 3269 (2004).
26. Y. Amao, *Microchim. Acta* **143**, 1 (2003).
27. S. Nagl, C. Baleizão, S. M. Borisov, M. Schäferling, M. N. Berberan-Santos, and O. S. Wolfbeis, *Angew. Chem. Int. Ed.* **46**, 2317 (2007).
28. G. Brusatin and P. Innocenzi, *J. Sol-Gel Sci. Technol.* **22**, 189 (2001).
29. O. S. Wolfbeis, *Anal. Chem.* **80**, 4269 (2008).